

# Evaluation of numerical method combinations for transport-dominated problems in the chemistry transport model (CHIMERE): Ozone prediction and Computing optimization study

Amine Ajdour (✉ [amine.ajdour@edu.uiz.ac.ma](mailto:amine.ajdour@edu.uiz.ac.ma))

University Ibn Zohr

Radouane Leghrib

University Ibn Zohr

Jamal Chaoufi

University Ibn Zohr

Ahmed Chirmata

Wilaya of Agadir

---

## Research Article

**Keywords:** Optimization, Ozone pollution, Transport chemistry model, computational performance, Transport dominated problems

**Posted Date:** March 28th, 2022

**DOI:** <https://doi.org/10.21203/rs.3.rs-1482337/v1>

**License:** © ⓘ This work is licensed under a Creative Commons Attribution 4.0 International License.

[Read Full License](#)

---

# **Evaluation of numerical method combinations for transport-dominated problems in the chemistry transport model (CHIMERE): Ozone prediction and Computing optimization study**

Amine Ajdour<sup>a\*</sup>, Radouane Leghrib<sup>a</sup>, Jamal Chaoufi<sup>a</sup>, Ahmed Chirmata<sup>b</sup>

<sup>a</sup>*LETSMP, Department of physics, Faculty of Sciences, University Ibn Zohr, Agadir, Morocco*

<sup>b</sup>*Department of energy and environment, Wilaya of Agadir, Agadir, Morocco*

*Corresponding author's email: amine.ajdour@edu.uiz.ac.ma*

## **Abstract.**

Ozone concentration generally affects a health system, including human health, and an ecosystem, including plant properties and soil processes. Based on high-performance computing, this study used the transport chemistry model CHIMERE to model ozone pollution in the city of Agadir. The aim is to investigate the integrating horizontal and vertical transport effect on ozone concentration and computation time. The findings are validated experimentally by measurements and also compared with other studies. The results highlighted four main points: First, the CHIMERE ozone modeling remains acceptable with a correlation coefficient of 70%. Second, the combination Adv00 based on the Upwind method gives good results in terms of ozone concentration with a significant implementation time, equivalent to 80 minutes for 360 hours of prediction, which means an optimization in computational performance. Third, it is required to optimize all possible parts of the modeling process to reduce costs and time. Fourth, detailed local emission information is recommended to get a clearer picture of the correction of the CHIMERE output. The present work can serve as guidance for the CHIMERE settings in the case of limited computational infrastructure for long-term studies and studies using a high spatial resolution to predict polluted air.

**Keywords: Optimization; Ozone pollution; Transport chemistry model; computational performance; Transport dominated problems.**

## 1. Introduction

Internationally, ozone is classified as a greenhouse gas (Gad, 2014; Simpson et al., 2014). The ozone control is informed by the World Health Organization guidelines and the United Nations Climate Change Convention (WHO, 2020). Ozone is a secondary pollutant caused by the chemical transformations under solar radiation of primary pollutants such as nitrogen oxides and volatile organic compounds (Visser et al., 2019). Ground-level ozone ( $O_3$ ) concentrations increased dramatically in the second half of the 20th century due to increased emissions of  $O_3$  precursors resulting from increased urbanization, severe industrial pollution, traffic emissions, agriculture, and energy consumption (Surya et al., 2020).

Ozone is a danger to both the ecosystem and health (Manisalidis et al., 2020). In ecological terms, ozone affects plant properties and soil processes that determine plant-soil-microbe interactions, such as soil enzyme activities and decomposition, leading to changes in soil ecosystem function (Andrady et al., 2017; Cisneros et al., 2010). Ozone also affects foliar chemistry and the formation of BVOC emissions, affecting insect-plant interactions (Pugh et al., 2013; Xu, 2021). In health terms, based on the results of several fields and clinical inhalation studies, significant health effects are expected if concentrations exceed  $240 \mu\text{g}/\text{m}^3$  for more than eight hours continuously (WHO, 2018). For example, healthy adults with asthma may experience a considerable decrease in lung function and airway inflammation, resulting in a profound deterioration of their health (Chen et al., 2018).

In recent years, modeling has proven powerful to predict various pollutants (Liu et al., 2021; Sofiev et al., 2013). As a result, they are widely used in scenario mining to test theories and understand the environmental impact under different emission rates, meteorological conditions, and development scenarios (Hosseiniebalam & Ghaffarpasand, 2015). The two main reasons for such use are on the one hand its efficiency and on the other hand its low cost and availability (Baklanov & Zhang, 2020). Depending on the algorithms adopted, there are different approaches to model air pollution (Mallet & Sportisse, 2008). The most commonly used air quality models can be divided into three main sections: diffusion modeling, photochemical modeling, and receptor modeling (Belis et al., 2020; Pino-Cortés et al., 2022; Ulfah et al., 2018).

Obtaining an accurate numerical simulation of ground-level ozone concentrations is a crucial challenge in air pollution (Todorov et al., 2020). The vertical and horizontal transport phenomena are essential for the flow dynamics study and simultaneously present a challenge for accurate numerical simulations and any new scheme development.

The main objective of this research is to improve the transport component in the CHIMERE model (Mailler et al., 2017). It should be noted that many studies have been conducted in this regard, implementing either the rational conservative scheme or the horizontal transport scheme only (Gavete et al., 2012; Hutchison & Mitchell, 2011). This study is not strange in this regard, during which the implementation of four numerical combinations from the numerical method is used in the horizontal and vertical transport. The results validation used similar studies and observations data in Agadir city.

Apart from the emissions and chemical process errors, the uniqueness of this work is the attempt to determine the integration effect of horizontal and vertical transport on ozone concentration and computational time. This paper is organized as follows: In Section 2, we present the model theory, the transport equation, and the finite volume methods that were evaluated. In Section 3,

we introduce the CHIMERE model setup and describe the results of this simulation. While section 4 discusses these results and attempts to interpret them, section 5 finally provides some conclusions.

## 2. Methodology

### 2.1. Data set and study area

Agadir is located in the Souss-Massa region in southern Morocco, situated on the northern side of the African continent (Bounoua et al., 2020). According to the Köppen Geiger classification, the Souss-Massa region has a warm Mediterranean climate with dry summers. The region is the first agricultural region of the country with a regional GDP of 17.3% and 9% and a total of 451,165 hectares of cultivated land, which makes it a sensitive area to air pollution. The air quality surveillance in the Agadir city is based on two measuring stations, a fixed ground station and a mobile regional station, both equipped with special SA environmental standards analyzers to detect harmful pollutants and climate variables (Chirmata et al., 2017). Data extraction is from the mobile station situated in the urban area of Anza in the study period from July 1 to July 15. This period was chosen in which the station is under the strict supervision of the Ministry of Interior, Department of Energy and Environment of the Province of Agadir because it provides continuous hourly data equivalent to 360 hours continuous.

### 2.2. CHIMERE concept

The evolution equation of chemical species concentrations ( $f_i$ ) can be decomposed into some individual factors, as illustrated in equation 1 (Menut et al., 2013). The species and meteorological variables are determined on the same grid. In the horizontal directions, the length of the grid cell is not significantly different from its neighbors. In the vertical dimension, the layer thickness increases exponentially with height.

$$\frac{\partial f_i}{\partial t} = \left(\frac{\partial f_i}{\partial t}\right)_{Advection} + \left(\frac{\partial f_i}{\partial t}\right)_{Turbulence} + \left(\frac{\partial f_i}{\partial t}\right)_{Chemistry} + \left(\frac{\partial f_i}{\partial t}\right)_{Emissions} + \left(\frac{\partial f_i}{\partial t}\right)_{Depot} \quad (1)$$

### 2.3. Transport equation

For realistic description, we started with the three-dimensional scalar advection problem (Goyal & Kumar, 2011). For each chemical species, the conservation equation is then numerically solved. ( $uf$ ) indicating the mass flow corresponding to  $u$  velocity.

$$\frac{\partial f}{\partial t} = -\nabla(uf) \quad (2)$$

This equation can be discretized and solved separately for each of the three orthogonal directions: zonal, meridian, and vertical, using the operator splitting technique and the CHIMERE design, including parallelepiped structured grids. This technique is more computationally and widely used in meteorological and chemistry-transport modeling. We notice  $\delta^\alpha(f)$ , the variation of ( $f$ ) due to transport in the direction  $\alpha$  and  $F$  is ( $uf$ ). After time and space discretization, the discretized transport calculations are as follows:

$$\delta^\alpha(f) = \left( \frac{(F)_{n+1/2}^\alpha - (F)_{n-1/2}^\alpha}{\Delta x} \right) \Delta t \quad (3)$$

The calculation of fluxes at cell interfaces ( $F_{n+1/2}^\alpha$ ) is a critical challenge in solving this equation. The characteristics of the transport scheme are determined by how these fluxes are numerically estimated. These numerical methods range from simple first-order numerical to higher-order methods. For simplicity, let's continue with a one-dimensional scalar advection problem for a typically atmospheric pollutant. we add an initial concentration  $f(x,0) = f_0$ , during the time interval  $[0, T]$ . The concentration of one typical pollutant is denoted by  $f$ . As a result, the description is the general Cauchy problem.

$$\begin{cases} \frac{\partial f}{\partial t} = \frac{\partial(uf)}{\partial x} & \forall (x, t) \in \mathbb{R} \times [0, T] \\ f(x, 0) = f_0 \end{cases} \quad (2)$$

## 2.4. Resolution Method

The analytical solution of air pollution equations is possible for simple cases. In the CHIMERE model, the finite volume approach is adopted (Mazumder, 2016). The conservative form of the transport equation in one dimension in space is solved using the finite volume method. Firstly, the spatial domain is divided into cells called control volumes. It corresponds to a partition of  $[0, L]$ , in one dimension. For time variable, let be  $[t^n, t^{n+1}]$  a uniform division of  $[0, T]$ , we designate time step as  $\Delta t = t^{n+1} - t^n$ . For space variable  $[x_{j-1/2}, x_{j+1/2}]$  is a division of  $[0, L]$ , we define space step as  $\Delta x = x_{j+1/2} - x_{j-1/2}$ , the control volume  $\Omega_j = [x_{j-1/2}, x_{j+1/2}]$ , and the center points  $x_j = \frac{x_{j+1/2} - x_{j-1/2}}{2}$ .

The integral form on each of the control volumes of the conservation law is given by:

$$\int_{\Omega_j} \frac{\partial f}{\partial t} dx = Q(f(x_{j-1/2}, t)) - Q(f(x_{j+1/2}, t)) \quad (5)$$

We note  $Q(f(x_{j-1/2}, t))$ ,  $Q(f(x_{j+1/2}, t))$ , the fluxes inside the cell. By integrating in time:

$$\int_{\Omega_j} f(x, t + \Delta t) - \int_{\Omega_j} f(x, t) = \int_t^{t+\Delta t} Q(f(x_{j-1/2}, t)) dt - \int_t^{t+\Delta t} Q(f(x_{j+1/2}, t)) dt \quad (6)$$

This term can be expressed as:

$$\gamma_j^{n+1} = \gamma_j^n - \frac{1}{\Delta x} (Q_{j+1/2}^n - Q_{j-1/2}^n) \quad (7)$$

where, we define the exact flux  $Q$  and the average values of the exact solution  $\gamma$  at time  $t$ , on each cell, we note  $F$ , the approximation of the function by:

$$\begin{cases} Q_{j+1/2}^n = \frac{1}{\Delta x} \int_t^{t+\Delta t} (uf)(x_{j+1/2}, t) dt \\ \gamma_j^n = \frac{1}{\Delta x} \int_{x_{j-1/2}}^{x_{j+1/2}} F(x, t) dx \end{cases} \quad (8)$$

$F$  est une fonction d'interpolation déterminée par l'algorithme conservatif. Cet article utilise trois approximations  $F$  distinctes, correspondant à des approximations constantes, linéaires et quadratiques de  $F$  sur chacune des cellules centrales. Dans la prochaine section, nous passerons en revue les trois options de transport disponibles dans le modèle.

### 2.4.1. Upwind Method

The upwind method uses a condition on the velocity sign to determine the advection concentration into the neighboring cell via the considered surface (Falcone & Ferretti, 2016). If  $u$  is positive, the moving wave solution of the equation above propagates to the right, with upwind referring to the left side, while downwind refers to the right side. If  $u$  is negative, the moving wave solution propagates to the left.

$$\begin{cases} \text{if } u > 0 & F_j(x) = \beta_j \\ \text{if } u < 0 & F_j(x) = \beta_{j-1} \end{cases} \quad (9)$$

For the CHIMERE model, the function  $f$  defined by  $f = \rho \cdot c$  with  $c$  is the concentration. Depending on the sign of the cell interface wind speed, the fluxes are described by the following equations:

$$\begin{cases} \text{if } u(t)_{j+1/2} > 0 & F_{j\pm 1/2} = \rho_j u_{j+1/2} c_j \\ \text{if } u(t)_{j+1/2} < 0 & Q_{j+1/2} = \rho_j u_{j+1/2} c_{j+1} \end{cases} \quad (10)$$

### 2.4.2. Van Leer Method

The Van Leer Method is a finite volume method for obtaining highly accurate numerical solutions for a given system, even when the solutions include shocks, discontinuities, or large gradient (Vanderheyden & Kashiwa, 1998). The concept is to use reconstructed states derived from cell-averaged states from the previous time step to replace the constant approximation of the Upwind method. For  $x \in \Omega_j$ , and taking into account the velocity  $u < 0$ .

$$F_j(x) = \beta_j + \alpha_j (x - x_{j-1/2}) \quad (11)$$

From the initial condition of each cell, we can determine the coefficient  $\beta_j$ :

$$\begin{cases} \text{if } u_{j+1/2} > 0 & F_j(x_{j-1/2}) = \beta_j = f_j \\ \text{if } u_{j+1/2} < 0 & F_j(x_{j-1/2}) = \beta_j = f_{j+1} \end{cases} \quad (12)$$

The concentration inside a grid cell is determined by a linear slope between the cell's two interfaces in the CHIMER model. It is a good compromise solution for long-range transport in meteorology between numerical accuracy and computational efficiency.

$$c_j(x) = \beta_j + (x - x_j)\alpha_j \quad (\text{Eq. 13})$$

With  $\beta_j = c_j$  and according to the following cases, the slope is calculated

$$\text{if } c_j \in [c_{j-1}, c_{j+1}] \quad \beta_j = \text{sign}(c_{j+1} - c_{j-1}) \times \min\left(\frac{c_{j+1} - c_{j-1}}{2\Delta x}, \frac{c_{j+1} - c_j}{\Delta x}, \frac{c_j - c_{j-1}}{\Delta x}\right) \quad (14)$$

### 2.4.3. Piecewise Parabolic Method (PPM)

Since PPM is a finite volume scheme, physical variables are represented as averages over a grid zone instead of single values at different points (Zhang et al., 2017). Then use the information from the average of the neighboring regions to fit a single monotonic parabola to the average

area of each dependent variable. PPM is a computational technique developed for fluid flow modeling with heavy impacts and discontinuities. It can handle steep gradients in small meteorological flows. For  $x \in \Omega_j$ , and taking into account the velocity  $u < 0$ . We note  $\bar{x}_j = (x - x_{j-1/2}) / \Delta x_j$ .

$$F_j(x) = \beta_j + \alpha_j x_j + \varphi_j x_j (1 - x_j) \quad (15)$$

The coefficients  $\beta_j$ ,  $\alpha_j$  and  $\varphi_j$  are obtained by the following formulas:

$$\begin{cases} \beta_j = F_j(x_{j-1/2}) \\ \alpha_j = F_j(x_{j+1/2}) - F_j(x_{j-1/2}) \\ \varphi_j = 6 \left( f_j - \frac{1}{2} (F_j(x_{j+1/2}) + F_j(x_{j-1/2})) \right) \end{cases} \quad (16)$$

Generally, this formula is directly applied to determine the flux function.

$$\begin{cases} \text{if } u(t)_{j+1/2} > 0 & Q_{j+1/2} = u_{j+1/2} \left( F_j(x_{j+1/2}) - \frac{u_{j+1/2} \Delta t}{2 \Delta x_j} \left( \Delta \beta_j - \left( 1 - \frac{2u_{j+1} \Delta t}{3 \Delta x_j} \right) \varphi_j \right) \right) \\ \text{if } u(t)_{j+1/2} < 0 & Q_{j+1/2} = u_{j+1/2} \left( F_{j+1}(x_{j+1/2}) - \frac{u_{j+1/2} \Delta t}{2 \Delta x_j} \left( \Delta \beta_{j+1} - \left( 1 - \frac{2u_{j+1} \Delta t}{3 \Delta x_{j+1}} \right) \varphi_{j+1} \right) \right) \end{cases} \quad (17)$$

### 3. Results

#### 3.1. Numerical experiments using CHIMERE model

Because an analytical expression for solving the chemical concentration evolution equation under realistic conditions is not available, it is not practical to directly determine the numerical errors in the 3D CTM simulation. Investigating the different superimposed phenomena equations' effect on air pollution is imperative to increase the modeling quality. This study follows the same approach so that ozone concentrations are predicted using the CHIMERE model based on four combinations of numerical solving transport-dominated equations. The CHIMERE model reliability is justified by comparing the results obtained with other studies or ground measurements. The model performance is evaluated based on three statistical metrics, including the correlation coefficient (R), mean bias (MB), and root means square error (RMSE), which are given by the formula in Table 1. Given M, O, and n are the modeled concentrations, the observed concentrations, the predictions or measurements number, respectively.

The Figure 1 illustrates the transport chemistry model general structure such as CHIMERE. For meteorology,  $u^*$  represents the frictional velocity,  $Q_0$  is the heat flux experienced at the surface, and BLH is the boundary layer height.  $[c]_{\text{CHIMERE}}$  and  $[c]_{\text{Obs}}$  are the modeled and observed concentrations, respectively. The modeling process was conducted using three fundamental models. The CHIMERE model, version 2017r3, calculate gas and aerosol concentrations based on WRF and Emis-surf data. Meteorological data is computed using the WRF (Weather Research Forecasting) model, version 4.0. Finally, the Emis-surf model, version 2016b, includes gas and aerosol emissions information.

The WRF advanced research model has been in ongoing development for several years. WRF can be used in numerous meteorological applications from meters to thousands of kilometers in scale (Dudhia, 2013). For data sets used in this model are available from the University Corporation for Atmospheric Research (UCAR). The CHIMERE model is a multi-scale Eulerian chemistry transport model. It is designed to generate daily pollutant forecasts, reproduce long-term emission scenarios, and study typical cases. This model depends on diverse inputs, such as meteorological conditions, land use, and emissions (A. Ajdour et al., 2019). The chemical boundary conditions are from the three-dimensional global chemistry-climate model LMDz-INCA, while the aerosol boundary conditions are from the GOCART and LMDz-AERO global models (Folberth et al., 2006). Anthropogenic emissions were estimated using the EDGAR-HTAP v2 2010 global emissions list (Ferreira et al., 2016). The horizontal resolution was set to 0.02° with 20 vertical levels in the troposphere ranging from 500 hPa to 200 hPa. The Figure 2 presents the WRF and CHIMERE domain.

Table 1. Statistical indicators formulas

Indicator	Formula
Correlation coefficient (r)	$\sum_{k=1}^n \frac{(M_k - \bar{M})(O_k - \bar{O})}{\sqrt{(M_k - \bar{M})^2} \sqrt{(O_k - \bar{O})^2}}$
Mean BIAS (MB)	$\frac{\sum_{k=1}^n (M_k - O_k)}{n}$
Root-Mean-Square Error (RMSE)	$\sqrt{\frac{\sum_{k=1}^n (M_k - O_k)^2}{n}}$

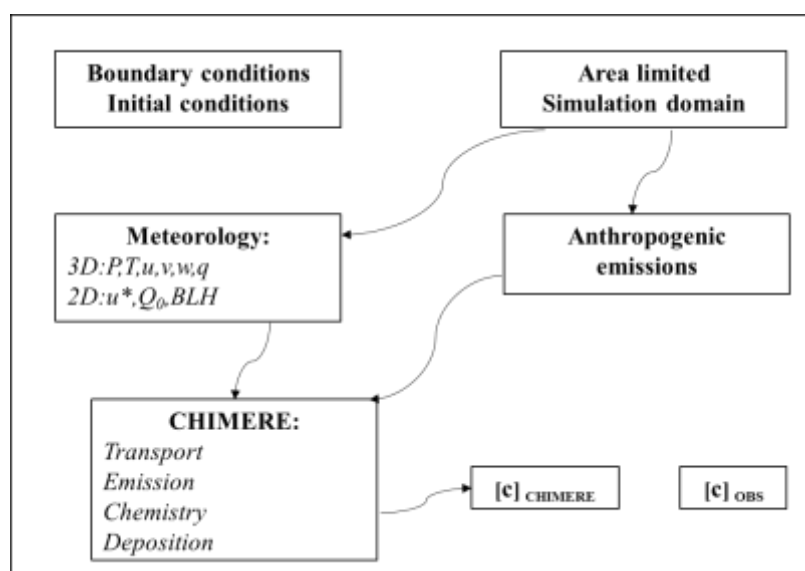


Figure 1. General structure of CHIMERE Model

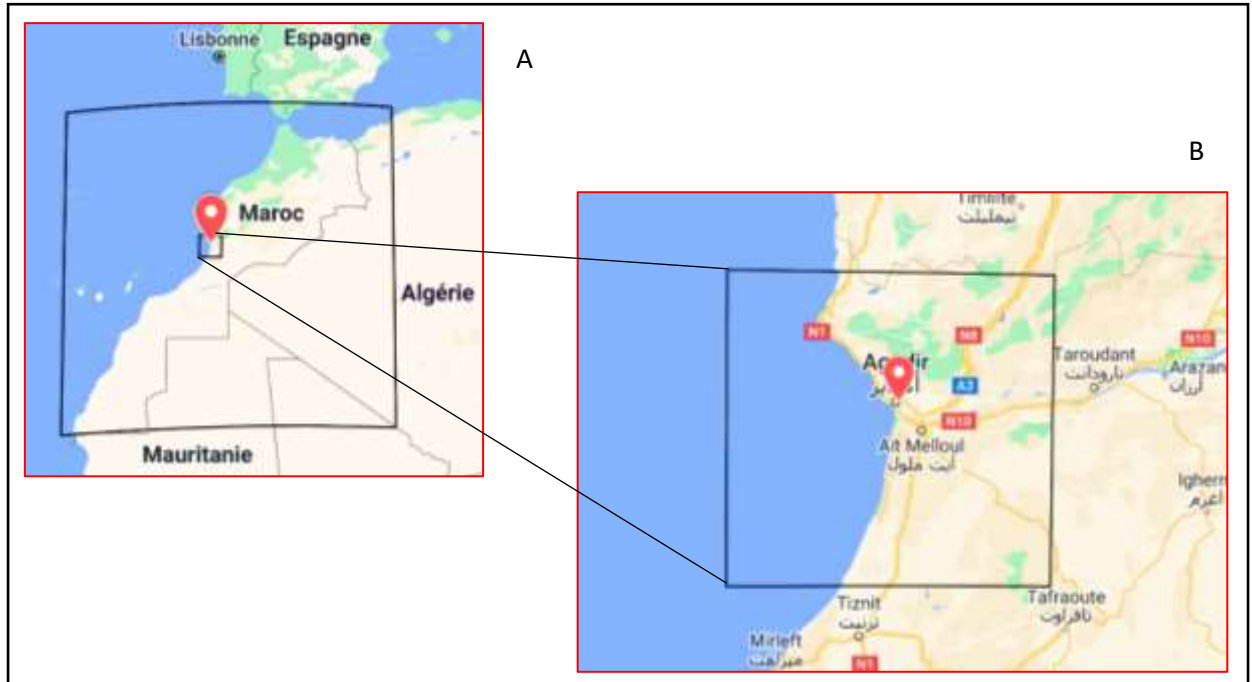


Figure 2. A) WRF's domain (large in black) and CHIMERE's domain (small in black) B) zoom of CHIMERE domain model

### 3.2. CHIMERE prediction positioning test

The Table 2 presents an analytical comparison of observed and modeled ozone over Agadir. The comparative data includes 360 hours of ozone concentrations from July 1, 2016. The measured ozone values ranged from 11.40 to 68.50  $\mu\text{g}/\text{m}^3$ , while the CHIMERE values ranged from 44.92 to 100.69  $\mu\text{g}/\text{m}^3$ . In statistics, the average is the measure of the central tendency of a given data. Measurements gave an average of 44.06  $\mu\text{g}/\text{m}^3$ , while CHIMERE showed an average peak of one and a half times that observed, reaching 69.96  $\mu\text{g}/\text{m}^3$ . For the dispersion data relative to the mean, the measurements and the CHIMERE model showed converging standard deviation values, up to 10.74  $\mu\text{g}/\text{m}^3$  for the observations and 9.83  $\mu\text{g}/\text{m}^3$  in the CHIMERE case.

Accurate and timely modeling with reduced computational time is essential to avoid the resulting risks and take appropriate action promptly pending supplementary support monitoring systems for future assessments. Generally, the CHIMERE model provides an overestimation of  $\sim 32.19 \mu\text{g}/\text{m}^3$  for the peak values recorded at midday with high solar radiation intensity. The nighttime overestimation, in which usually the ozone concentration should be lower, is estimated to be about 33.52  $\mu\text{g}/\text{m}^3$ . We conclude that CHIMERE's ozone gas modeling is still limited, especially during peak and night hours, consistent with other studies (Ascenso et al., 2021; De Meij et al., 2009). We can note from the standard deviation that the data are clustered for models and measurements similarly. For eight consecutive hours, the World health organization limit is 100  $\mu\text{g}/\text{m}^3$  (Chiquetto et al., 2019). The model exceeded this limit in some ozone peaks, while the measurements did not exceed it.

The Figure 3 presents the time series of the average hourly  $\text{O}_3$  concentration for CHIMERE and the observation of the city of Agadir. This figure clearly shows the strong trend between

CHIMERE and the measurement. It also displays a tendency for both to increase throughout the study. The first line of Table 5 shows the calculated statistical parameters for the current study.

In particular, the correlation coefficient indicates that the model maintains the trend despite the significant bias coefficient indicating the difficulty of predicting using CHIMERE. Against the observations, the hourly correlations show a correlation of 70%; as a result, the model performs well to the Russell and Dennis criteria (Russell & Dennis, 2000), the same thing this statistical score meets the Emery criteria (Emery et al., 2017). Regarding MB and RMSE, we could not determine the extent of their compliance with the Russell and Dennis (2000) and Emery (2017) criteria based on their dependence on other statistical scores. The previously mentioned criteria were based on cutoff values ranging from 40  $\mu\text{g}/\text{m}^3$  to 60  $\mu\text{g}/\text{m}^3$ , and other studies reached 80  $\mu\text{g}/\text{m}^3$ , which were excluded from this study. Ozone cutoff values varied from study to study, while the U.S. Environmental Protection Agency sets a limit of 60 ppb to measure the overall error (USEPA, 2015). The choice of cutoff values is to investigate the effect of higher concentrations on human health effects. The cutoff values are helpful to select the dangerous concentrations and remove the influence of low concentrations such as nighttime values (Arasa et al., 2012). At the same time, it does not give a clear idea of the modeling quality. The problem of various cutoffs from different comparisons complicates the overall interpretation of the modeled results.

The Table 3 shows the statistical parameters calculated for the CHIMERE model compared to three other studies. The first study used in this comparison investigates the CHIMERE model performance in Agadir city in Morocco using two resolutions, C1 ( $0.1^\circ=11$  km) and C3 ( $0.02^\circ=2$  km). The obtained numerical results are compared with spring and summer ozone monitoring data from 2010. The second study provides a quantitative performance evaluation and a better understanding of the potential shortcomings of the WRF-Polyphemus modeling system used to simulate air quality in Lebanon for the most common gaseous pollutants (CO, NO<sub>2</sub>, O<sub>3</sub>, SO<sub>2</sub>) as well as for the particulate species (PM<sub>10</sub>, PM<sub>2.5</sub>, EC<sub>2.5</sub>, OC<sub>2.5</sub>). The third study evaluates the NMMB/BSC-CTM online model by simulating the main gaseous pollutant concentrations in Europe for the year 2010. The model results are evaluated with ground-based observations, ozone probes, and satellite retrievals.

Compared to the other three studies, the results showed a good correlation coefficient, which indicates that the model maintains the trend. As for the MB, we do not hide the fact that the third study gave the lowest value of MB compared to CHIMERE, as it is close to the value obtained in Study 2. Concerning the RMSE, the result is approximately the same as the one obtained in the third study. Comparing the results of the present study with the first study, which in turn was conducted on Moroccan, in Agadir city using CHIMERE, the current correlation coefficient is good despite the presence of MB and RMSE differences.

The results obtained remain acceptable and consistent with the three approved studies. Although this comparison validated the results to further the study purpose, the differences are due to two main reasons: the different locations of each study and the methods adopted in the modeling process. As a clarification, the distinction between the current study and the first study is that the first study relied on 2010 data obtained from the fixed station, while the present study relied on 2016 measurements from a mobile station, Requires updating the spatial-temporal analysis to represent air quality monitoring stations (Baca-López et al., 2021). We can confirm

from this study conducted in the same city that the large MB observed is associated with low nitrogen dioxide concentrations (Brancher, 2021). The CHIMERE discrepancy is generally associated with the lower resolution of the emissions information at each time step derived from the annual totals in the HTAP inventory database. Moreover, the model's horizontal accuracy is  $0.02^\circ$ , while the stations record very local values for the data (de Meij et al., 2009). Therefore, detailed information about the local emissions is recommended to get a clearer picture to correct the CHIMERE output, which we will do now.

The Table 4 summarizes the four combinations selected for this study based on the numerical method used for horizontal and vertical transport. The Table 5 represents the effect of these combinations on the ozone results using four statistical factors. The correlation coefficient effect does not exceed 1%, while the mean bias and RMSE reach  $0.72 \text{ ug/m}^3$  and  $0.84 \text{ ug/m}^3$ , respectively, switching from adv00 and adv21. Although congruence appeared significantly between all combinations, Figure 4 shows alternative views of the average hourly concentration differences with adv00 as the reference compared to the other formulations listed in Table 4. To determine delta1, delta2 and delta 3, we calculate the following differences  $\text{delta1} = C_{\text{Adv10}} - C_{\text{Adv00}}$ ,  $\text{delta2} = C_{\text{Adv11}} - C_{\text{Adv00}}$  and  $\text{delta3} = C_{\text{Adv21}} - C_{\text{Adv00}}$ . According to Figure 4, the difference in concentration appears in the night period at 10 pm and from 2 am to 3 am. In the morning period from 7 am to 8 am, while in the night period precisely at 3 pm. For the computation time, significant differences appear, up to 80 minutes as a difference between adv00 and adv21. In other words, about 45% of the execution time using adv00, giving a representative ratio for this metric.

In general, the statistical comparison of the numerical method combinations shows close statistical results without any significant differences affecting ozone concentrations. Using the Adv 00 method as a reference, the most pronounced deviations are observed at midday during the peak ozone period, at 3:00 pm, when the gap does not exceed  $2 \text{ ug/m}^3$ . These findings are in good agreement with other studies investigating the same subject (Gavete et al., 2012; Hutchison & Mitchell, 2011), although they mainly neglect the effect of numerical method combinations on modeling time. A significant difference was observed in the execution time, which showed a time difference of 80 minutes for 360 hours of prediction. Adopting the same computational capacities in this investigation, over a study of one year, the difference, in this case, will be about 1946 minutes, which is equivalent to 32.43 hours. All simulations were performed using a remotely accessible high-performance computing (HPC) infrastructure (Kornyei et al., 2021) provided by the National Center for Scientific and Technical Research to the Moroccan research community. The infrastructure contains 19 nodes with the following capacity, 760 processor cores, 108 TB of storage, 5.2 TB of RAM, and 2 GPUs. This infrastructure is connected to a 5Gbps link to ensure high data transfer speeds from attached universities and institutions. The computational time is a decisive element in any modeling work (Nibart et al., 2021), which depends heavily on numerical methods and computational infrastructure. In this case, the Adv00 combination based on the Upwind method represents the optimal solution to the vertical and horizontal transport equation. According to the results of this study, it is categorically recommended to use the adv00 combination, especially for high spatial resolution, as in this study ( $0.02^\circ$ ), as the high resolution in the CHIMERE model requires a high computational time and a robust computational infrastructure.

Table 2. Characteristics of measured and modeled ozone

	<b>O<sub>3</sub>(OBS)</b>	<b>O<sub>3</sub> (CHIMERE)</b>
<b>Range [Min; Max] [ug/m<sup>3</sup>]</b>	[11.40 ; 68.50]	[44.92 ; 100.69]
<b>Average [ug/m<sup>3</sup>]</b>	44.06	69.96
<b>Standard Deviation [ug/m<sup>3</sup>]</b>	10.74	9.83
<b>Missing data [%]</b>	0	0

Table 3. Statistical parameters calculated for the CHIMERE model compared to three other studies.

	<b>Model</b>	<b>Study area</b>	<b>Correlation</b>	<b>Mean bias [ug/m<sup>3</sup>]</b>	<b>RMSE [ug/m<sup>3</sup>]</b>	<b>Ref</b>
<b>Present study</b>	CHIMERE	Morocco	70%	25.90	27.09	-
<b>Study 1</b>	CHIMERE	Morocco	61%	13.60	13.93	(Amine Ajdour et al., 2022)
<b>Study 2</b>	Polyphemus	Lebanon	60%	25.70	38.60	(Abdallah et al., 2018)
<b>Study 3</b>	NMMB/BSC-CTM	Europe	60%	4.80	27.08	(Badia & Jorba, 2015)

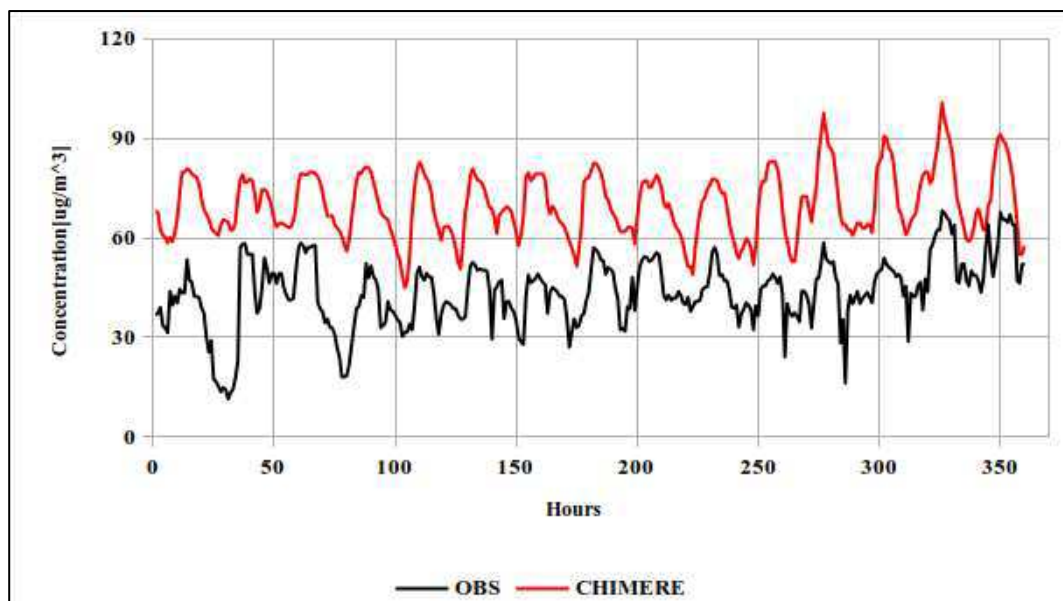


Figure 3. Hourly time series of measured and modeled ozone

Table 4. The four combinations depending on the numerical method used during horizontal and vertical transport

		Horizontal		
		Upwind (0)	PPM (1)	Van Leer (2)
Vertical	Upwind (0)	Adv00	Adv10	-
	Van Leer (1)	-	Adv11	Adv21

Table 5. The ozone evaluation of each combination studied

	Correlation	Mean bias	RMSE	Running time
<b>Adv00</b>	70%	25.90	27.09	178.42
<b>Adv10</b>	69%	26.24	27.53	238.84
<b>Adv11</b>	69%	26.57	27.90	255.54
<b>Adv21</b>	70%	26.62	27.93	259.01

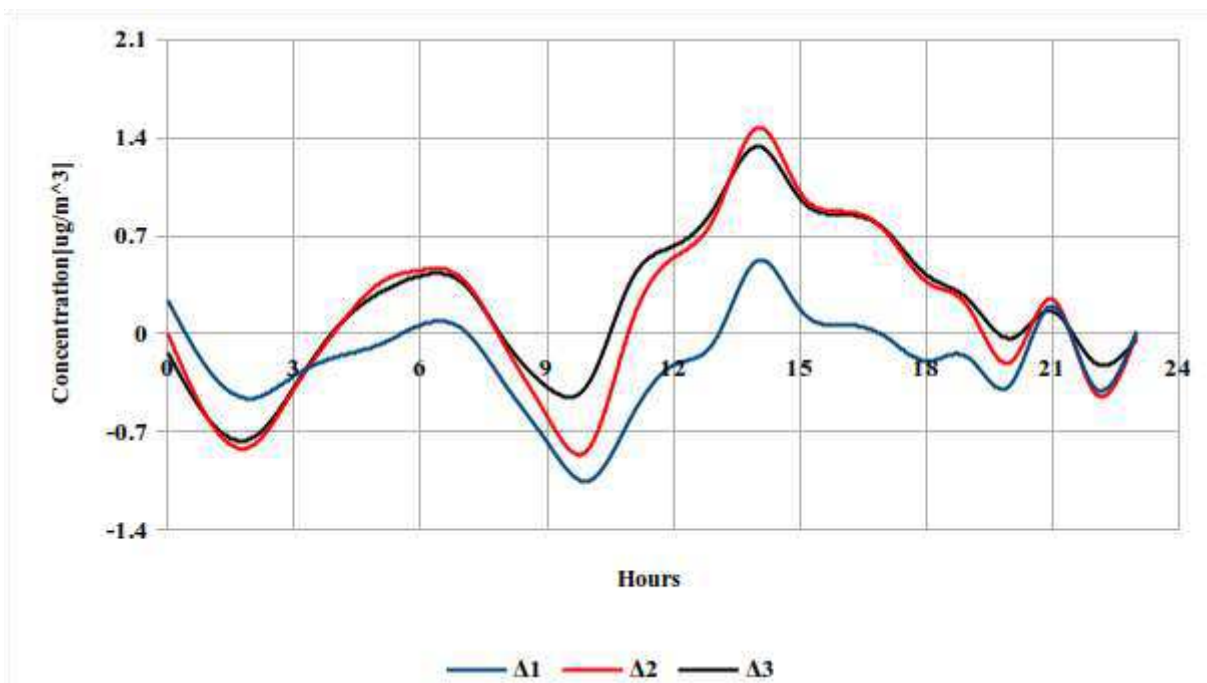


Figure 4. The daily deltas between adv10, adv11 and Adv21 using Adv00 as a reference

## Conclusion

Air quality forecasting has been a concern for the scientific community in recent years. The main goal of this study is to improve the chemical transport component in the CHIMERE model using four combinations determined by numerical methods used in horizontal and vertical transport. Although the combination types examined did not affect the ozone concentration, they constituted a critical element in the modeling time determination. In addition to accuracy, the latter is one of the foundations of modeling. The results conclusively showed that the combination (Adv00) based on the Upwind method gives good results similar to other formulations in terms of ozone concentration while saving a significant amount of run-time, which means saving computing power. The results highlighted the value of understanding the

combined effects of the algorithm employed to simulate the transport phenomenon. As applications, this study can be used in all future modeling processes to prepare the CHIMERE model, especially studies using high spatial resolution or long-term studies based on limited computational infrastructure to predict air pollution. Finally, it can be adopted for a large-scale application and refers to a series of future studies.

### **Acknowledgments**

The Faculty of Science University Ibn Zohr supported this research in all its stages. We would like to thank warmly Ministry of Interior, especially the department of energy and Environment of the Souss Massa region, for their collaboration. We are grateful to the Dynamic Meteorology Laboratory (LMD) for its valuable assistance. The calculations for this simulation were done using the national HPC managed by the National Center of Scientific and Technological Research (CNRST) in Morocco. The authors are grateful to the staff of “HPC” in particular Ms. Bouchra RAHIM, a computer engineer, for her availability and assistance with computer work.

### **Availability of data and materials**

The datasets used and/or analyzed during the current study are available from the corresponding author on reasonable request.

### **Funding declaration**

This research received no specific grant from any funding agency in the public, commercial, or not-for-profit sectors.

### **Conflicts of Interest Statement**

All authors certify that they have no affiliations with or involvement in any organization or entity with any financial interest or non-financial interest in the subject matter or materials discussed in this manuscript.

### **Author Contribution**

**Amine Ajdour:** Methodology, Investigation, writing – original draft, Writing – review & editing, Formal analysis. **Radouane Leghrib:** Supervision, Data acquisition, Writing – review & editing, Formal analysis. **Jamal Chaoufi:** Supervision, Conceptualization, Methodology, Formal analysis. **Ahmed Chirmata:** Formal analysis, Data acquisition, Conceptualization.

### **References**

- Abdallah, C., Afif, C., El Masri, N., Öztürk, F., Keleş, M., & Sartelet, K. (2018). A first annual assessment of air quality modeling over Lebanon using WRF/Polyphemus. *Atmospheric Pollution Research*, 9(4), 643–654. <https://doi.org/10.1016/j.apr.2018.01.003>
- Ajdour, A., Leghrib, R., Chaoufi, J., Chirmata, A., Menut, L., & Mailler, S. (2019). Towards air quality modeling in Agadir City (Morocco). *Materials Today: Proceedings*, xxx. <https://doi.org/10.1016/j.matpr.2019.07.438>
- Ajdour, Amine, Leghrib, R., Chaoufi, J., & Chirmata, A. (2022). High spatial resolution effect on ozone pollution modelling: Case study of Agadir city (Morocco). *Materials Today:*

*Proceedings*, 52, 137–141. <https://doi.org/10.1016/j.matpr.2021.11.278>

- Andrady, A., Aucamp, P. J., Austin, A. T., Bais, A. F., Ballaré, C. L., Barnes, P. W., Bernhard, G. H., Björn, L. O., Bornman, J. F., Erickson, D. J., De Gruijl, F. R., Häder, D. P., Ilyas, M., Longstreth, J., Lucas, R. M., Madronich, S., McKenzie, R. L., Neale, R., Norval, M., ... Zepp, R. G. (2017). Environmental effects of ozone depletion and its interactions with climate change: Progress report, 2016. *Photochemical and Photobiological Sciences*, 16(2), 107–145. <https://doi.org/10.1039/c7pp90001e>
- Arasa, R., Soler, M. R., & Olid, M. (2012). Evaluating the Performance of a Regional-Scale Photochemical Modelling System: Part I—Ozone Predictions. *ISRN Meteorology*, 2012, 1–22. <https://doi.org/10.5402/2012/860234>
- Ascenso, A., Gama, C., Blanco-Ward, D., Monteiro, A., Silveira, C., Viceto, C., Rodrigues, V., Rocha, A., Borrego, C., Lopes, M., & Isabel Miranda, A. (2021). Assessing douro vineyards exposure to tropospheric ozone. *Atmosphere*, 12(2), 1–17. <https://doi.org/10.3390/atmos12020200>
- Baca-López, K., Fresno, C., Espinal-Enríquez, J., Martínez-García, M., Camacho-López, M. A., Flores-Merino, M. V., & Hernández-Lemus, E. (2021). Spatio-Temporal Representativeness of Air Quality Monitoring Stations in Mexico City: Implications for Public Health. *Frontiers in Public Health*, 8(January), 1–15. <https://doi.org/10.3389/fpubh.2020.536174>
- Badia, A., & Jorba, O. (2015). Gas-phase evaluation of the online NMMB/BSC-CTM model over Europe for 2010 in the framework of the AQMEII-Phase2 project. *Atmospheric Environment*, 115, 657–669. <https://doi.org/10.1016/j.atmosenv.2014.05.055>
- Baklanov, A., & Zhang, Y. (2020). Advances in air quality modeling and forecasting. *Global Transitions*, 2, 261–270. <https://doi.org/10.1016/j.glt.2020.11.001>
- Belis, C. A., Pernigotti, D., Pirovano, G., Favez, O., Jaffrezo, J. L., Kuenen, J., Denier van Der Gon, H., Reizer, M., Riffault, V., Alleman, L. Y., Almeida, M., Amato, F., Angyal, A., Argyropoulos, G., Bande, S., Beslic, I., Besombes, J. L., Bove, M. C., Brotto, P., ... Yubero, E. (2020). Evaluation of receptor and chemical transport models for PM10 source apportionment. *Atmospheric Environment: X*, 5(November 2019), 100053. <https://doi.org/10.1016/j.aeaoa.2019.100053>
- Bounoua, L., Fathi, N., El Berkaoui, M., El Ghazouani, L., & Messouli, M. (2020). Assessment of Sustainability Development in Urban Areas of Morocco. *Urban Science*, 4(2), 18. <https://doi.org/10.3390/urbansci4020018>
- Brancher, M. (2021). Increased ozone pollution alongside reduced nitrogen dioxide concentrations during Vienna's first COVID-19 lockdown: Significance for air quality management. *Environmental Pollution*, 284(2), 117153. <https://doi.org/10.1016/j.envpol.2021.117153>
- Chen, H., Li, Q., Kaufman, J. S., Wang, J., Copes, R., Su, Y., & Benmarhnia, T. (2018). Effect of air quality alerts on human health: a regression discontinuity analysis in Toronto, Canada. *The Lancet Planetary Health*, 2(1), e2–e3. [https://doi.org/10.1016/S2542-5196\(17\)30185-7](https://doi.org/10.1016/S2542-5196(17)30185-7)
- Chiquetto, J. B., Silva, M. E. S., Cabral-Miranda, W., Ribeiro, F. N. D., Ibarra-Espinosa, S. A., & Ynoue, R. Y. (2019). Air quality standards and extreme ozone events in the São Paulo megacity. *Sustainability (Switzerland)*, 11(13), 1–14.

<https://doi.org/10.3390/su11133725>

- Chirmata, A., Leghrib, R., & Ichou, I. A. (2017). Implementation of the Air Quality Monitoring Network at Agadir City in Morocco. *Journal of Environmental Protection*, 08(04), 540–567. <https://doi.org/10.4236/jep.2017.84037>
- Cisneros, R., Bytnerowicz, A., Schweizer, D., Zhong, S., Traina, S., & Bennett, D. H. (2010). Ozone, nitric acid, and ammonia air pollution is unhealthy for people and ecosystems in southern Sierra Nevada, California. *Environmental Pollution*, 158(10), 3261–3271. <https://doi.org/10.1016/j.envpol.2010.07.025>
- De Meij, A., Gzella, A., Cuvelier, C., Thunis, P., Bessagnet, B., Vinuesa, J. F., Menut, L., & Kelder, H. M. (2009). The impact of MM5 and WRF meteorology over complex terrain on CHIMERE model calculations. *Atmospheric Chemistry and Physics*, 9(17), 6611–6632. <https://doi.org/10.5194/acp-9-6611-2009>
- de Meij, A., Thunis, P., Bessagnet, B., & Cuvelier, C. (2009). The sensitivity of the CHIMERE model to emissions reduction scenarios on air quality in Northern Italy. *Atmospheric Environment*, 43(11), 1897–1907. <https://doi.org/10.1016/j.atmosenv.2008.12.036>
- Dudhia, J. (2013). Overview of WRF physics. *WRF Workshop 2013*, 1–207. <https://doi.org/10.1016/j.atmosres.2014.12.019>
- Emery, C., Liu, Z., Russell, A. G., Odman, M. T., Yarwood, G., & Kumar, N. (2017). Recommendations on statistics and benchmarks to assess photochemical model performance. *Journal of the Air and Waste Management Association*, 67(5), 582–598. <https://doi.org/10.1080/10962247.2016.1265027>
- Falcone, M., & Ferretti, R. (2016). Numerical Methods for Hamilton–Jacobi Type Equations. In *Handbook of Numerical Analysis* (1st ed., Vol. 17). Elsevier B.V. <https://doi.org/10.1016/bs.hna.2016.09.018>
- Ferreira, M. F. G., Curci, G., & Lanfri, M. (2016). First Implementation of the WRF-CHIMERE-EDGAR Modeling System Over Argentina. *IEEE Journal of Selected Topics in Applied Earth Observations and Remote Sensing*, 9(12), 5304–5314. <https://doi.org/10.1109/JSTARS.2016.2588502>
- Folberth, G. A., Hauglustaine, D. A., Lathièrel, J., & Brocheton, F. (2006). Interactive chemistry in the Laboratoire de Météorologie Dynamique general circulation model: Model description and impact analysis of biogenic hydrocarbons on tropospheric chemistry. *Atmospheric Chemistry and Physics*, 6(8), 2273–2319. <https://doi.org/10.5194/acp-6-2273-2006>
- Gad, S. C. (2014). Ozone. *Encyclopedia of Toxicology: Third Edition*, 3, 747–750. <https://doi.org/10.1016/B978-0-12-386454-3.00895-2>
- Gavete, L., Vivanco, M. G., Molina, P., Gavete, M. L., Urena, F., & Benito, J. J. (2012). Implementation in CHIMERE of a conservative solver for the advection equation-cmmse10. *Journal of Computational and Applied Mathematics*, 236(12), 3026–3033. <https://doi.org/10.1016/j.cam.2011.04.003>
- Goyal, P., & Kumar, A. (2011). Mathematical Modeling of Air Pollutants: An Application to Indian Urban City. *Air Quality-Models and Applications*. <https://doi.org/10.5772/16840>
- Hosseiniabalam, F., & Ghaffarpasand, O. (2015). The effects of emission sources and

- meteorological factors on sulphur dioxide concentration of Great Isfahan, Iran. *Atmospheric Environment*, 100, 94–101. <https://doi.org/10.1016/j.atmosenv.2014.10.012>
- Hutchison, D., & Mitchell, J. C. (2011). (*Lecture Notes in Computer Science 6785*) *Svajūnas Sajavičius (auth.), Beniamino Murgante, Osvaldo Gervasi, Andrés Iglesias, David Taniar, Bernady O. Apduhan (eds.) - Computational Science and I.pdf*.
- Kornyei, L., Horvath, Z., Ruopp, A., Kovacs, A., & Liszkai, B. (2021). *Multi-scale Modelling of Urban Air Pollution with Coupled Weather Forecast and Traffic Simulation on HPC Architecture*. 9–10. <https://doi.org/10.1145/3440722.3440917>
- Liu, H., Yan, G., Duan, Z., & Chen, C. (2021). Intelligent modeling strategies for forecasting air quality time series: A review. *Applied Soft Computing*, 102, 106957. <https://doi.org/10.1016/j.asoc.2020.106957>
- Mailler, S., Menut, L., Khvorostyanov, D., Valari, M., Couvidat, F., Siour, G., Turquety, S., Briant, R., Tuccella, P., Bessagnet, B., Colette, A., Létinois, L., Markakis, K., & Meleux, F. (2017). CHIMERE-2017: From urban to hemispheric chemistry-transport modeling. *Geoscientific Model Development*, 10(6), 2397–2423. <https://doi.org/10.5194/gmd-10-2397-2017>
- Mallet, V., & Sportisse, B. (2008). *Air quality modeling : From deterministic to stochastic approaches*. 55, 2329–2337. <https://doi.org/10.1016/j.camwa.2007.11.004>
- Manisalidis, I., Stavropoulou, E., Stavropoulos, A., & Bezirtzoglou, E. (2020). Environmental and Health Impacts of Air Pollution: A Review. *Frontiers in Public Health*, 8. <https://doi.org/10.3389/fpubh.2020.00014>
- Mazumder, S. (2016). Unstructured Finite Volume Method. In *Numerical Methods for Partial Differential Equations: Vol. M*. <https://doi.org/10.1016/b978-0-12-849894-1.00007-x>
- Menut, L., Bessagnet, B., Khvorostyanov, D., Beekmann, M., Blond, N., Colette, A., Coll, I., Curci, G., Foret, G., Hodzic, A., Mailler, S., Meleux, F., Monge, J.-L., Pison, I., Siour, G., Turquety, S., Valari, M., Vautard, R., & Vivanco, M. G. (2013). CHIMERE 2013: a model for regional atmospheric composition modelling. *Geoscientific Model Development*, 6(4), 981–1028. <https://doi.org/10.5194/gmd-6-981-2013>
- Nibart, M., Ribstein, B., Ricolleau, L., Tinarelli, G., Barbero, D., Albergel, A., & Moussafir, J. (2021). Optimization of hpc use for 3d high resolution urban air quality assessment and downstream services. *Atmosphere*, 12(11). <https://doi.org/10.3390/atmos12111410>
- Pino-Cortés, E., Carrasco, S., Acosta, J., de Almeida Albuquerque, T. T., Pedruzzi, R., & Díaz-Robles, L. A. (2022). An evaluation of the photochemical air quality modeling using CMAQ in the industrial area of Quintero-Puchuncavi-Concon, Chile. *Atmospheric Pollution Research*, 13(3). <https://doi.org/10.1016/j.apr.2022.101336>
- Pugh, T. A. M., Ashworth, K., Wild, O., & Hewitt, C. N. (2013). Effects of the spatial resolution of climate data on estimates of biogenic isoprene emissions. *Atmospheric Environment*, 70, 1–6. <https://doi.org/10.1016/j.atmosenv.2013.01.001>
- Russell, A., & Dennis, R. (2000). NARSTO critical review of photochemical models and modeling. *Atmospheric Environment*, 34(12–14), 2283–2324. [https://doi.org/10.1016/S1352-2310\(99\)00468-9](https://doi.org/10.1016/S1352-2310(99)00468-9)
- Simpson, D., Arneth, A., Mills, G., Solberg, S., & Uddling, J. (2014). Ozone - the persistent menace: Interactions with the N cycle and climate change. *Current Opinion in*

*Environmental Sustainability*, 9–10, 9–19. <https://doi.org/10.1016/j.cosust.2014.07.008>

- Sofiev, M., Siljamo, P., Ranta, H., Linkosalo, T., Jaeger, S., Rasmussen, A., Rantio-Lehtimäki, A., Severova, E., & Kukkonen, J. (2013). A numerical model of birch pollen emission and dispersion in the atmosphere. Description of the emission module. *International Journal of Biometeorology*, 57(1), 45–58. <https://doi.org/10.1007/s00484-012-0532-z>
- Surya, B., Hamsina, H., Ridwan, R., Baharuddin, B., Menne, F., Fitriyah, A. T., & Rasyidi, E. S. (2020). The complexity of space utilization and environmental pollution control in the main corridor of Makassar City, South Sulawesi, Indonesia. *Sustainability (Switzerland)*, 12(21), 1–41. <https://doi.org/10.3390/su12219244>
- Todorov, V., Kandilarov, J., Dimov, I., & Vulkov, L. (2020). High-accuracy numerical methods for a parabolic system in air pollution modeling. *Neural Computing and Applications*, 32(10), 6025–6040. <https://doi.org/10.1007/s00521-019-04088-x>
- Ulfah, S., Awalludin, S. A., & Wahidin, W. (2018). Advection-diffusion model for the simulation of air pollution distribution from a point source emission. *Journal of Physics: Conference Series*, 948(1). <https://doi.org/10.1088/1742-6596/948/1/012067>
- USEPA. (2015). *Air Quality Modeling Technical Support Document for the 2008 Ozone NAAQS Cross-State Air Pollution Rule Proposal* (Issue November).
- Vanderheyden, W. B., & Kashiwa, B. A. (1998). Compatible Fluxes for van Leer Advection. *Journal of Computational Physics*, 146(1), 1–28. <https://doi.org/10.1006/jcph.1998.6070>
- Visser, A. J., Folkert Boersma, K., Ganzeveld, L. N., & Krol, M. C. (2019). European NO<sub>x</sub> emissions in WRF-Chem derived from OMI: Impacts on summertime surface ozone. *Atmospheric Chemistry and Physics*, 19(18), 11821–11841. <https://doi.org/10.5194/acp-19-11821-2019>
- WHO. (2018). WHO | Air pollution and health: Summary. *WHO*. <https://www.who.int/airpollution/ambient/about/en/>
- WHO. (2020). *Air pollution*. [https://www.who.int/health-topics/air-pollution#tab=tab\\_1](https://www.who.int/health-topics/air-pollution#tab=tab_1)
- Xu, X. (2021). Recent advances in studies of ozone pollution and impacts in China: A short review. *Current Opinion in Environmental Science and Health*, 19, 100225. <https://doi.org/10.1016/j.coesh.2020.100225>
- Zhang, W., Wang, T., Bai, J. S., Li, P., Wan, Z. H., & Sun, D. J. (2017). The piecewise parabolic method for Riemann problems in nonlinear elasticity. *Scientific Reports*, 7(1), 1–17. <https://doi.org/10.1038/s41598-017-13484-z>